

## Analysis and design of structural elements of an industrial steel warehouse with overhead crane

Arthur Almeida Cordeiro de Farias\*, Douglas Mateus de Lima\*, Iálysson da Silva Medeiros\*, Henrique Tavares Lima\*, Pablo Aníbal López-Yáñez \*\*

\* (Center for Technology, Graduate Program in Civil and Environmental Engineering, Federal University of Pernambuco, Caruaru-PE, Brazil

\*\* (Department of Civil and Environmental Engineering, Federal University of Pernambuco, Recife-PE, Brazil

### ABSTRACT

Advancing the growth and expansion of industries requires faster, more efficient, economical and durable construction. Allied to this, the need for transportation and lifting of loads inside industrial warehouses has become increasingly greater, without the loss of physical storage space. A very efficient way to solve this problem is the use of overhead cranes. This work consists of the design and verification of an industrial steel warehouse with an overhead crane, in which the warehouse's constituent elements were verified, as well as the bearing beam that supports the bridge. The static analysis of the structure was performed with the aid of the SAP 2000 software, which provided the active requests, and the displacement of the structural elements. The wind-related actions acting on the structure were determined in accordance to the Brazilian norm. The structural checks were made based on the criteria established by other Brazilian norms. The base plates of the shed columns were dimensioned using criteria and methods established in Steel Design Guide 1. Finally, the connections between the bottom chord and the bayonet and between the top chord and the bayonet are presented. **Keywords** - Industrial warehouse. Overhead crane. Rolling beam. Structural analysis.

Date of Submission: 09-02-2022

Date of Acceptance: 23-02-2022

### I. INTRODUCTION

The sheds are generally single-story constructions, which have large covered areas and are intended for commercial, industrial, agricultural and other purposes. In the industrial sector, there is often a need to transport and lift loads inside the sheds and, for this, it is necessary to use auxiliary equipment, such as overhead cranes. Furthermore, advancing the growth and expansion of industries requires faster constructions that are efficient, economical and durable. For this reason, the use of steel sheds becomes viable.

Historical evidence shows that the use of cargo handling equipment emerged from the 1st century AD, in which, later on, the use of this equipment was more widespread for the construction of European cathedrals, still in the Middle Ages [1].

However, the most used system in the handling and lifting of loads in industries, mainly due to the

lack of space, which limits the amount of machinery arranged inside the shed, is the overhead crane.

According to [2], overhead cranes are equipment used in the transport and lifting of loads, generally with high capacities and high duty cycles. It is a structure, normally installed inside buildings, being possible to move loads, materials, equipment, among others, in the longitudinal, transversal and vertical directions, without reducing the useful storage area.

With the use of overhead cranes, it is possible to reduce costs with labor and materials, in addition to improving the working conditions of employees. In this way, the implementation of overhead cranes in industrial warehouses increases the productive capacity of the area, as it will increase the internal space available for stock and movement of materials and equipment.

The use of overhead cranes in industrial warehouses has been the subject of several analyzes carried out by researchers. Studies carried out by [3] can be highlighted, who developed a control scheme

for the sliding mode of a three-dimensional crane, with the objective of regulating the position and anti-oscillation control; [4] established an anti-sway control method for overhead cranes; [5] that evaluated the straightness condition of an crane bridge in a metallic structure; [6] who developed an overhead crane emergency braking method; [7] carried out an analysis of the damage caused by fatigue of a steel truss that supported an overhead crane; [8] who performed a dynamic analysis and determined an optimized anti-swing control of the crane time; and [9] who proposed a lightweight design method that meets the principles of overhead crane design, based on the multi-specular reflection algorithm.

Thus, in order to meet the demand of the industrial sector and the advantages that the use of an overhead crane can bring, this work will analyze and dimension the structural elements of an industrial steel shed with the use of an overhead crane, as well as present the methodologies for analysis and verification of a project of this type.

## II. DESCRIPTION OF THE STUDY SHED

The industrial shed under study has 20,000 mm of transversal span and 42,000 mm of longitudinal span, 9,000 mm of column and more 4,000 mm of bayonet. The roof is formed by a gabled truss with galvanized steel tiles. The top of the overhead crane bearing beam is at a height of 9,800 mm. In Fig. 1, the elevation of this shed and the indications of each constituent element are presented, with dimensions in millimeters.

Longitudinally, the shed is composed of eight frames and, consequently, seven spans, each span being spaced at 6,000 mm and the bracings placed in the central span, as can be seen in Fig. 2, with dimensions in millimeters.

The fact that the vertical bracings are made in the central span has advantages and disadvantages. The advantage is that there are no concerns with the addition of actions due to temperature variation in the structure, while the disadvantage is that all lateral actions that act on the end wall girts must travel through the horizontal struts to the lateral bracing system.

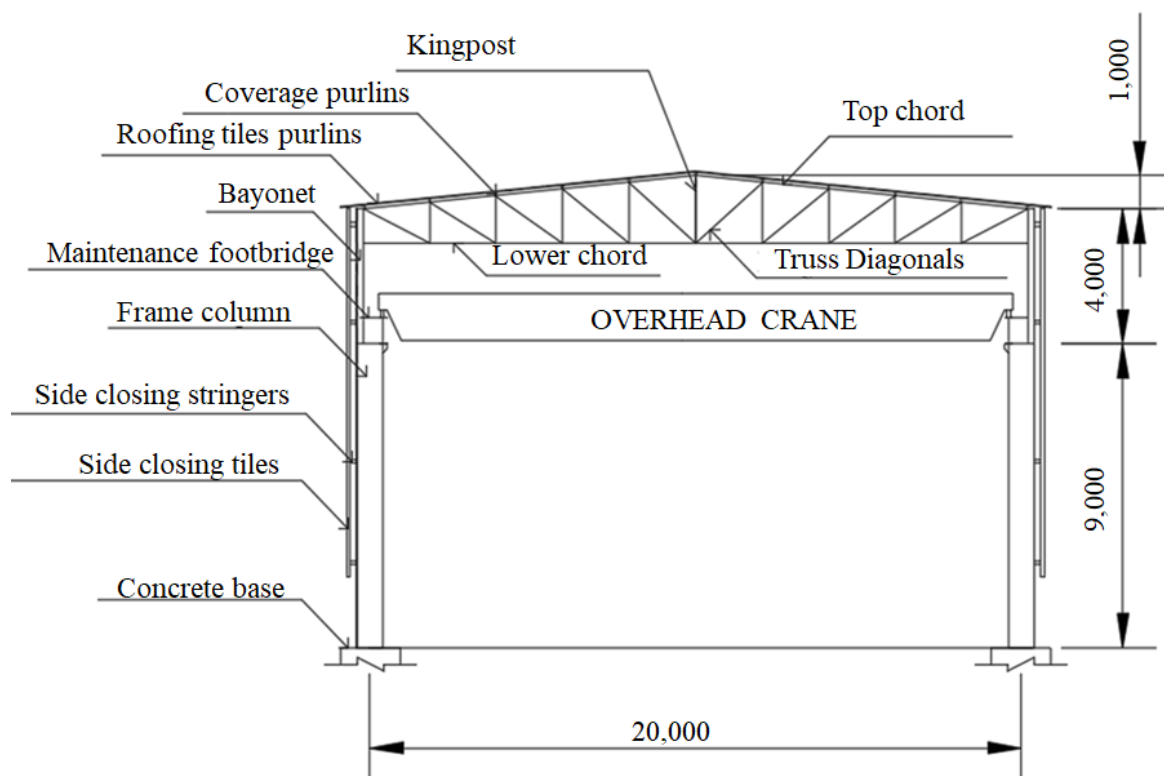
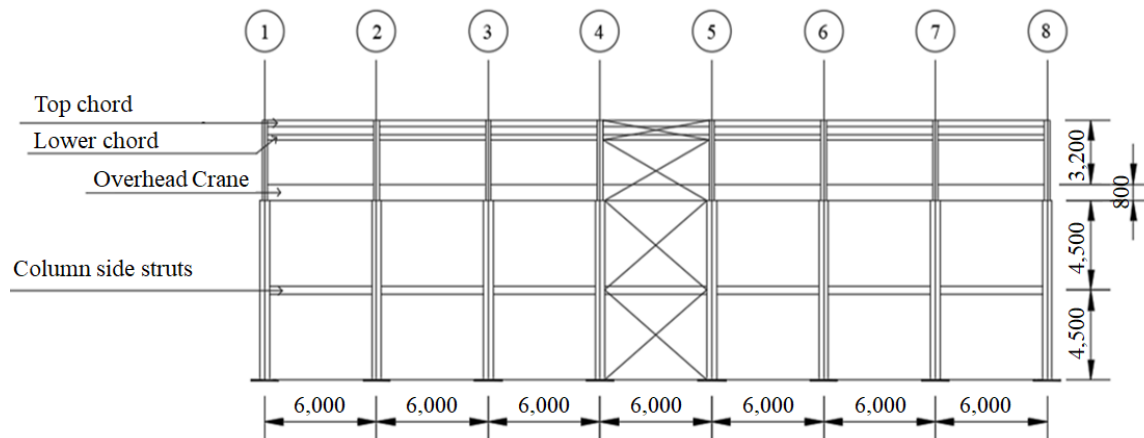


Fig. 1: Front elevation of the studied shed.



**Fig. 2: Lateral elevation of the studied shed.**

For the purpose of lateral containment to the buckling of the compressed bars and slenderness of the tensioned bars, which must meet the service limit states, the bracing system of the roof and bottom chord was defined, where the points contained laterally in the trusses are determined. For the bracing of the bottom chord of the truss, struts will be used at every two nodes, which will also receive the horizontal actions transmitted from the end wall

girts columns, in addition to a central bracing system, between the trusses of axes 4 and 5.

The cover bracing will be used to reduce the buckling length in the top chord of the trusses and to support a small lateral force in the closing region of the trusses, this being a light bracing. Stream lines will be installed on the purlins, spaced 2 m apart, also with the aim of reducing the buckling length. In Fig. 3, the roof plan is presented, where the elements mentioned above are highlighted.

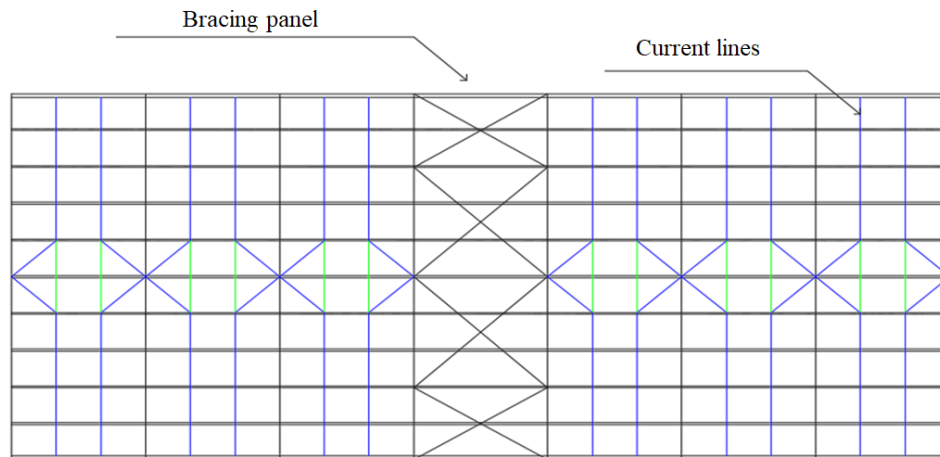


**Fig. 3: Roof bracing panel and current lines.**

The bearing beam will receive longitudinal actions, due to the braking of the bridge itself, as well as transverse actions, due to the braking of the trolley. When there are longitudinal actions, the bearing beam will serve as an element for transmitting the efforts to the central bracing. The braking force due to the trolley must be supported by the gantry, composed of columns, trusses and

bayonets, and the gantry must have strength and stability for this situation.

### III. STRUCTURAL ANALYSIS SOFTWARE

For structural analysis and launching of the loads acting on the structure, the SAP 2000 student software was used, which is a software for static and dynamic, linear and non-linear structural analysis,

using finite elements, in which a plane frame was modeled and the appropriate active actions.

Linear static analysis of the structural elements was performed and the software was extracted, after launching the calculation combinations, the

envelopes of the forces acting on the structure and the deformations of the structural elements.

#### IV. LOAD COMBINATIONS

The dead load, initially estimated, that act uniformly on the structure, are presented in Table 1.

Table 1: Deadloads in the structure.

Dead load	Acting weight
Trusses own weight	0.058 kN m <sup>-2</sup>
Own weight of purlins and stringers	0.039 kN m <sup>-2</sup>
Own weight of tie rods and crossarm braces	0.020 kN m <sup>-2</sup>
Own weight of tiles - e = 0.66mm	0.070 kN m <sup>-2</sup>
Upper column self-weight ("bayonet")	0.700 kN m <sup>-1</sup>
Lowercolumn self-weight	1.100 kN m <sup>-1</sup>
Bearingbeam self-weight	0.900 kN m <sup>-1</sup>
Own weight of rails (TR 32) and accessories	0.400 kN m <sup>-1</sup>
Own weight of the maintenance footbrigde (checkered plate 6 mm)	0.670 kN m <sup>-2</sup>
Self-weight of the side beam of the walkway (U 152 mm x 12.2 kg/m)	0.120 kN m <sup>-1</sup>

For the use and occupation overload, Annex B of [10] establishes that in common roofs, not subject to accumulation of any materials, and in the absence of specification to the contrary, a minimum nominal overload of 0.25 kN m<sup>-2</sup>, in horizontal projection. To be more in favor of safety, a nominal overload of 0.50 kN m<sup>-2</sup> to the roof, and a uniformly distributed overload over the maintenance walkway equal to 3.00 kN m<sup>-2</sup>.

As for the actions due to the wind, for the shed under study, a basic speed was considered, V<sub>0</sub>, equal to 30 m.s<sup>-1</sup>, a topographical factor, S<sub>1</sub> equal to 1, the terrain being approximately flat, a statistical factor, S<sub>3</sub>, equal to 1, and a terrain roughness factor, S<sub>2</sub>,

calculated for different heights, according to item 5.3 of [11]. For a height of 5 m, the roughness factor is equal to 0.76, for 9 m it presents the value of 0.82, for 13 m and 14 m, the terrain roughness factors are equal to 0.86 and 0.87, respectively.

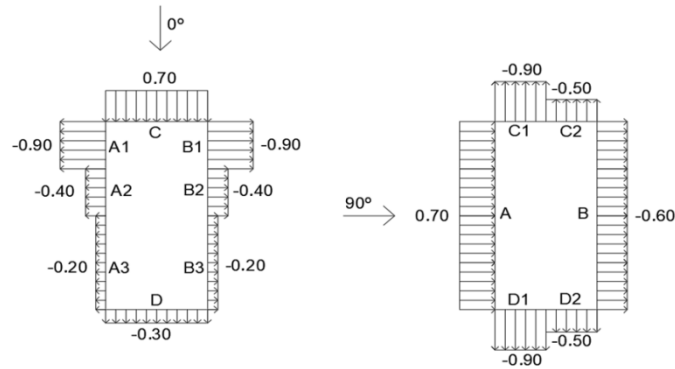
For the calculation of the characteristic speeds and dynamic pressures of the wind acting on the structure, the four heights mentioned in the previous paragraph were considered and according to item 4.2 of [11], being, for the last two levels, a single pressure value, because the two are very close. The values of speeds and pressures are presented in Table 2.

Table 2: Characteristic wind speeds and dynamic pressures.

Height (m)	Characteristic speed (m.s <sup>-1</sup> )	Dynamic pressure (kN m <sup>-2</sup> )
5	22.8	0.32
9	24.6	0.37
13	25.8	0.42
14	26.1	0.42

Through the parameters of the shed under study and the criteria established in item 6.1 of [11], it was possible to determine the pressure coefficients and

external shape, for the wind incident at 0° and 90°, in the entire perimeter of the side coverings, the which are shown in Fig. 4.



**Fig. 4: External shape coefficients on the side blinds for wind at 0° and 90°.**

The pressure and shape coefficients for the roof were obtained from Table 5 of [11].

Fig. 5 shows the coefficients obtained for winds at 0° and 90°.

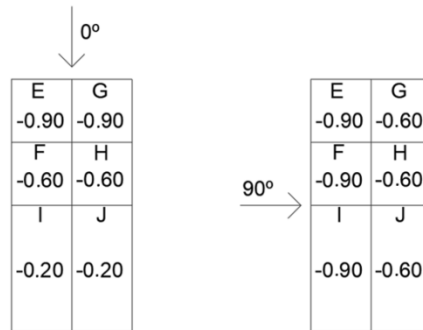


**Fig. 5: External pressure coefficients in the cover for wind at 0° and 90°.**

According to [11], for permeable buildings, the internal pressure can be considered uniform. For this building, four equally permeable faces were considered, because, despite the existence of lateral closings, the spaces between the tiles and the closing masonry allow the partial passage of the wind, which generates an internal pressure coefficient,  $c_{pi}$ ,

equal to -0.3 or 0, both for 0° and 90° wind, and the most critical value should be considered.

The combinations of the external pressure and shape coefficients with the internal pressure coefficients, with wind at 0°, are shown in Fig. 6 and Fig. 7, only for regions EG and IJ, which are the most critical cases.

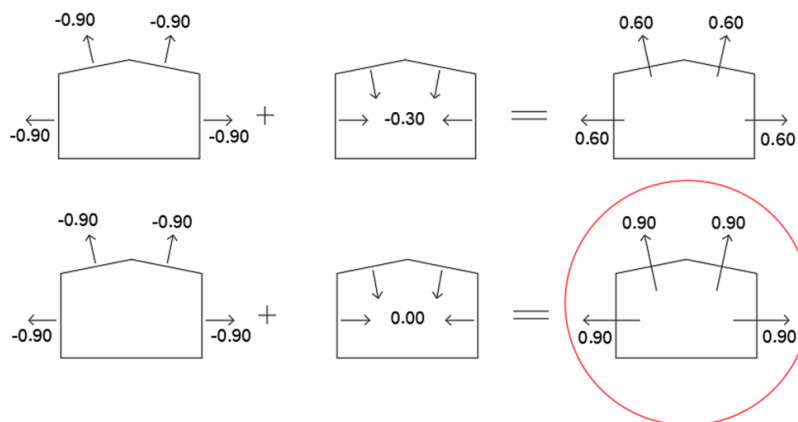


**Fig. 6: Combinations of coefficients in the EG region for wind at 0°.**

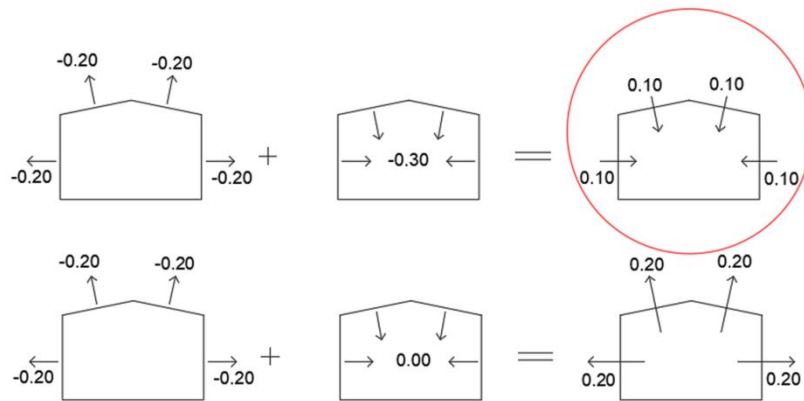


**Fig. 7: Combinations of coefficients in region IJ for wind at 0°.**

In Fig. 6 and Fig. 7, the most unfavorable combination for the stability of the structure is highlighted, with 0.10 being the highest value of overpressure and 0.9 the highest value of suction.

For 90° wind the combinations are the same in all regions and are represented in Fig. 8.

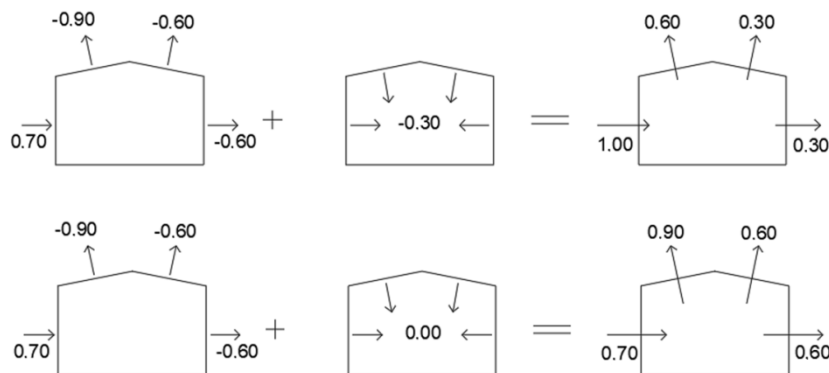


**Fig. 8: Combinations of coefficients for 90° wind.**

For this situation, it is not possible to visually identify the most unfavorable combination, therefore, the structure calculation must be carried out for the two wind situations. Therefore, four situations of actions due to wind in the structure will be considered.

In addition to these combinations, the combinations of actions due to wind in the end wall shed will also be considered, to calculate the end wall columns and the metallic elements that are part of the central bracing.

For design the bearing beam, it is necessary to know the type train of the crane, which is supplied by the crane manufacturer. According to the manufacturer, the maximum load of the type train that acts on the overhead crane, at the moment when the trolley is as close as possible to one of the ends is  $P_{\text{máx}} = 163 \text{ kN}$ , while the minimum load on the other

head is  $P_{\text{mín}} \sim 0.4 P_{\text{máx}} = 65.2 \text{ kN}$ . These loads include the total load that the bridge can hoist, the self-weight of the bridge, the self-weight of the trolley and the self-weight of the entire crane mechanism.

To calculate the maximum bending moment that acts on the rolling beam, Equation 1 is used, which was obtained through the study of the influence line for the bending moment in the bearing beam.

$$M_{\text{máx}} = \frac{\varphi P}{2l} \left(1 - \frac{a}{2}\right)^2 \quad (1)$$

being,  $P$  is the load that the crane exerts on the bearing beam;  $\varphi$  is the vertical impact coefficient of the crane;  $l$  is the length of the bearing beam;  $a$  is the distance between the two wheels at the head of the bridge.

The [10] in its annex B, recommends as a vertical impact coefficient for this type of crane the value of 1.25.

In addition to the bending moment, there is a horizontal force longitudinal to the runway, caused by the bridge braking, and a horizontal transverse force, caused by the trolley braking. Item B.7.2 of Annex B of [10] recommends, in cases where the manufacturer does not provide the values of these horizontal forces, the approximation presented in Equations 2 and 3.

$$H_t \sim 0.1 P_{\text{vert}} \quad (2)$$

$$H_l \sim 0.2 P_{\text{máx}} \quad (3)$$

being,  $H_t$  is the force transverse to the rolling path, acting on the top of the rails;  $P_{\text{vert}}$  is the sum of the lifted load plus the weight of the trolley and lifting devices;  $H_l$  is the force longitudinal to the bearing path;  $P_{\text{máx}}$  is the maximum vertical load of each crane wheel, without using the vertical impact coefficient.

## V. RESULTS AND DISCUSSIONS

This item presents the determinations of requests and verifications of the structural elements of the shed, such as columns, bayonets, truss bars, purlins, stringers and bearing beam, in addition to their respective connections.

In the case of columns and bayonets, which are elements subject to flexure and compression, a second-order analysis of the structure must be

carried out. For this work, an approximate second-order analysis was performed, according to Annex D of [10].

### 5.1. COVERING TRUSSES

In this item, the combinations of actions acting on the trusses will be presented, as well as the results of the dimensioning of the chords, diagonals and amounts. These elements were dimensioned considering the LRFD (Load and Resistance Factor Design) load combinations, following the criteria of [10], using ASTM A36 steel.

#### 5.1.1. Loads on trusses

The project in question presents three different types of variable actions acting on the frames, they are: the actions due to the wind, the occupation overload and the actions caused by the crane. From these actions, both the wind and the crane can act in four different ways on the structure. This makes possible a great number of possibilities of performances, simultaneous or not, of these actions.

For all load cases there are 308 possible combinations of actions, associated with their corresponding weighting and combination coefficients presented in item 4.7.6 of [10], however, through a critical analysis, it was possible to determine that 80 of these combinations could be more harmful to the structure.

Table 3 shows the LFRD load combinations of the load groups used in this work.

Table 3: Combinations of actions acting on the gantry.

Combination group	Load groups with their coefficients	Number of combinations
1	1.25 DL + 1.5 LL	1
2	1.25 DL + 1.4 W	4
3	1.0 DL + 1.4 W	3
4	1.25 DL + 1.5 CR	4
5	1.25 DL + 1.5 CR + 0.75 LL	4
6	1.25 DL + 1.5 LL + 1.05 CR	4
7	1.25 DL + 1.5 LL + 0.84 W + 1.05 CR	4
8	1.25 DL + 1.5 CR + 0.75 LL + 0.84SV	16
9	1.25 DL + 1.4 W + 0.75 LL + 1.05 CR	16
10	1.0 DL + 1.4 W + 1.05 CR	12
11	1.0 DL + 1.4 W + 0.75 LL + 1.05 CR	12

being DL is the dead load; SC the live load of use and occupation; W actions due to wind; CR the actions of the crane over the gantry.

The combinations were launched in the frame of the calculation model in the SAP 2000 software and, through this, it was possible to obtain the load

envelopes. Then, the bars were dimensioned in terms of tensile and compressive strengths.

#### 5.1.2. Tensile and compressive strengths of the bars

For constructive reasons, the same profile was adopted for each type of truss element. The verification of the design resistant axial force for the tensile stresses was made considering the yield of the gross section and the rupture of the net section, according to item 5.2.2 of [10].

The axial compressive strength of calculation was determined according to item 5.3 of [10]. It was observed that, except for the uprights, none of the profiles dimensioned in tension would resist the compression acting on the truss bars; thus, for this verification, the axial compression forces requesting and resistant to the calculation, as well as the profiles dimensioned and verified for each element are presented in Table 4.

Table 4: Verification of compressive strength and final design of profiles.

<b>Top chord</b>				
Designation:	$N_{c,Rd}$ (kN)	Section	$N_{c,Sd}$ (kN)	Use of the designation
2L 2 ½ in x 3/16 in	151.37	7 - 8	138.48	91.48%
<b>Bottom chord</b>				
Designation:	$N_{c,Rd}$ (kN)	Section	$N_{c,Sd}$ (kN)	Use of the designation
2L 3 in x 3/16 in	141.64	21 - 22	112.48	79.41%
<b>Post</b>				
Designation:	$N_{c,Rd,max}$ (kN)	Section	$N_{c,Sd,max}$ (kN)	Use of the designation
2L 1 ½ in x 1/8 in	60.38	2 - 13	56.12	92.95%
<b>Diagonals</b>				
Designation:	$N_{c,Rd,max}$ (kN)	Section	$N_{c,Sd,max}$ (kN)	Use of the designation
2L 2 ½ in x 3/16 in	132.95	11 - 21	126.13	94.87%

being,  $N_{c,Rd}$  the axial compressive strength of calculation resistant;  $N_{c,Sd}$  is axial compressive force design requesting;  $N_{c,Rd,max}$  is the design resistant axial compressive force for the most requested profile, on posts and diagonals;  $N_{c,Sd,max}$  is the axial compressive force required for the calculation for

the most requested profile, in the posts and diagonals.

Checking the slenderness of each profile, the number of clips and the distance between them for all the trusses elements were calculated, as shown in Table 5.

Table 5: Truss double angle profile clips.

<b>Top chord</b>				<b>Bottom chord</b>			
Section	L (cm)	n	$l_{ef}$ (cm)	Section	L (cm)	n	$l_{ef}$ (cm)
All	201	3	50.25	All	200	2	66.67
<b>Posts</b>				<b>Diagonals</b>			
Section	L (cm)	n	$l_{ef}$ (cm)	Section	L (cm)	n	$l_{ef}$ (cm)
2 - 13	120	3	30.00	1 - 13	224	3	56.00
3 - 14	140	3	35.00	2 - 14	233	3	58.25
4 - 15	160	3	40.00	3 - 15	244	3	61.00
5 - 16	180	3	45.00	4 - 16	256	3	64.00
6 - 17	200	3	50.00	5 - 17	269	3	67.25
7 - 18	180	3	45.00	7 - 17	269	3	67.25
8 - 19	160	3	40.00	8 - 18	256	3	64.00
9 - 20	140	3	35.00	9 - 19	244	3	61.00
10 - 21	120	3	30.00	10 - 20	233	3	58.25
				11 - 21	224	3	56.00

being, L is the length of the profile; n is the number of loops;  $l_{ef}$  is the distance between the clamps.

The distances between the clamps presented in Table 5 were calculated according to the

recommendation of item 5.2.8.2 of [10], which says “that profiles or plates, separated from each other by a distance equal to the thickness of spacer plates, be interconnected through these spacer plates, so that the highest slenderness index of any profile or plate, between these connections, does not exceed 300”.

## 5.2. COLUMNS AND BAYONETS

In this item, the results obtained in the design and verification of the columns that make up the frame, the bayonets and the end wall columns will be presented. These three elements undergo the same types of requests, and the same checks are made for them. The elements were checked for compressive strength, flexural compression and shear strength in the ultimate limit state, in addition to giving an

approximate second-order analysis for the second case. The steel considered for the design of these elements was ASTM A36.

### 5.2.1. Requesting Efforts

Because the columns are subject to three different types of stresses, they must be checked for all the ultimate normal combinations which cause maximum values of these stresses. Through the results obtained from the SAP 2000 software, it was verified that, for the columns that make up the frame, there are three combinations of actions which cause maximum values of efforts of each type, while for the bayonet, a single combination generated these maximum values. The results obtained are shown in Table 6.

Table 6: Critical combinations on frame columns and bayonets.

Structural frame columns					
Type of effort	Combination	P (kN)	V (kN)	M (kN m)	
$P_{m\acute{a}x}$ (AXIAL)	1.25 DL +1,5 CR <sub>4</sub> + 0,75 LL + 0,84 W <sub>2</sub>	528.22	46.17	260.09	
$V_{m\acute{a}x}$ (SHEAR)	1.25 DL +1,5 CR <sub>4</sub> + 0,75 LL + 0,84 W <sub>4</sub>	499.87	56.07	312.54	
$M_{m\acute{a}x}$ (MOMENT)	1.25 DL +1,5 CR <sub>2</sub> + 0,75 LL + 0,84 W <sub>3</sub>	293.23	42.16	366.46	
Bayonets					
$P_{m\acute{a}x}$ , $V_{m\acute{a}x}$ e $M_{m\acute{a}x}$	1.25 DL +1.5 LL + 0.84 W <sub>2</sub> + 1.05 CR <sub>2</sub>	86.43	86.57	86.47	

being, CR<sub>4</sub> the action of the crane in case the trolley is on the right side, with braking to the same side; CR<sub>2</sub> if the trolley is on the left side, with braking to the right; W<sub>2</sub> is the overpressure wind at 0°; W<sub>3</sub> is the first case of wind at 90°; W<sub>4</sub> is the second case of wind at 90°.

The end wall columns are not requested to the same actions as the frames, only the actions due to the wind, the self-weight and the dead load of the roofing tiles and stringers act on them, therefore, it presents a unique critical combination of the ultimate limit state, in which the wind is considered the main variable. For this, the maximum bending moment acting on the end wall column of 36 kN m, the maximum shear force of 13 kN and the maximum axial force of 13 kN were calculated.

### 5.2.2. Column and bayonet profiles

The profiles of each element are initially estimated for later verification of compliance with the criteria established in [10], always looking for the lightest profile that can fulfill all requirements, generating savings and security. For the verifications of this work, a WB (Welded Beam)

800 mm x 111 kg/m profile was considered for the gantry columns, a BCW (Beam Column Welded) 400 mm x 82 kg/m profile for the bayonets and a CW (Column Welded) 250 mm x 43 kg/m profile for the end wall columns. The reason for using a WB profile for the frame columns is the fact that there is a need for a larger dimension of this column in the direction transverse to the bearing path, to support the bearing beam, in addition to the need for the profile to have a greater inertia in the same direction, to resist the horizontal forces caused by the trolley braking.

### 5.2.3. Buckling coefficients of the mixed column-bayonet section

When cross-section and/or normal force variation occurs, greater mathematical difficulties arise in obtaining the buckling load in the frame plane. To obtain the buckling coefficients of the columns and bayonets, the method proposed by [12] was used for bars with sudden cross-sectional variation and normal force, with one end free and the other fixed.

The buckling coefficients in the shear plane obtained through this method for the columns were equal to 2.115 and for the bayonets equal to 7.648. However, according to [13], no buckling coefficient value ever tried was greater than 3. In view of this, the buckling coefficient of the bayonet around the x axis was considered equal to 3.

#### 5.2.4. Approximate 2<sup>nd</sup> order analysis

The displacement analysis for all the LFRD load combinations of actions performed by the SAP 2000 software generated results for the relationship between the lateral displacements in the second-order and first-order analyzes of less than 1.1, which characterizes, according to item 4.9.4.2 of the [10], a structure of small displacement.

In structures of small displacement, according to item 4.9.7.1.4 of [10], the global second-order effects can be disregarded if,

a) the axial forces requesting the calculation of all the bars whose flexural stiffness contributes to the lateral stability of the structure, in each of the LFRD load combinations of actions stipulated in 4.7.7.2, do not exceed 50% of the axial force corresponding to the yielding of the section transversal of these bars;

b) the effects of the initial geometric imperfections are added to the respective combinations, including those in which variable actions due to the wind act.

The elements that give the portico lateral stability are the columns and bayonets. The axial force corresponding to the yielding of the column cross section is equal to 3,550 kN, while for the bayonet this value is equal to 2,625 kN. The proportions between the maximum axial forces acting and the axial forces that correspond to the yielding of the section are equal to 15% for the columns and 3% for the bayonets, which are less than the 50% limit.

For these considerations, a horizontal force equivalent to 0.3% of the value of the design gravitational loads applied to all columns according to item 4.9.7.1.1 of [10] should be applied, as initial geometric imperfections. These effects can be understood as a minimal lateral loading of the structure and are not combined with the other horizontal actions. In this work, the gantry presents horizontal actions much greater than the notional

actions, as seen in item 2.3 of this work, the horizontal action of the crane is equivalent to 10% of the vertical force, which leads to the conclusion that any combination with these actions notional would not be critical.

The second order local effects were considered by amplifying the bending moments by the amplification factor  $B_1$ , calculated according to Annex D of [10]. Therefore, depending on the considerations seen above, the global second-order effects can be disregarded. Thus, the amplification factors for the second-order local effects were calculated, with values of 1.086 and 1.046 being obtained for the respective combinations of maximum axial force and maximum bending moment in the frame columns, 1.011 for the bayonets and 1.015 for the columns from end wall.

#### 5.2.5. Verification of metal profiles

Through the analysis of the envelope of efforts obtained in SAP 2000, it was observed that, for certain combinations of calculation, tensile efforts can be generated in the columns of the frame and in the bayonets, however, the value of such effort is negligible if compared to the efforts of compression. Therefore, the verification of the design resistant tensile axial force was neglected.

The determination of the axial compressive strength of calculation was obtained following the same procedure adopted for the truss bars in item 3.1.2 of this work, according to item 5.3 of [10].

To verify the bending acting on the columns and bayonets, the design resistant bending moments were determined according to Annex G of [10] for non-slender web beams and were verified taking into account the ultimate limit states of Lateral-Torsional Buckling (LTB), Web Local Buckling (WLB), Flange Local Buckling (FLB), in addition to other criteria established in item 5.4.2 of [10].

The columns and bayonets were also checked to flexure and compression, according to item 5.5.1 of [10], considering the amplification factors of bending moments due to second-order effects, presented in item 3.2.4 of this work.

The design resistant shear forces were calculated according to item 5.4.3.1 of [10], considering that there is no transverse stiffener along the entire length.

The results obtained for all the aforementioned checks on the frame columns, bayonets and end wall columns, with their respective requesting and

resistant calculation efforts, are presented in Table 7, together with the use of the profile for each check.

Table 7: Verification of the profiles.

<b>Frame Columns</b>			
Compression	$N_{c,Sd}$ (kN) 528.22	$N_{c,Rd}$ (kN) 2090.86	25.26%
Flexion	$M_{Sd}$ (kN m) 366.46	$M_{Rd}$ (kN m) 630.7	58.10%
Flexure and compression combination			67.80%
Shear	$V_{Sd}$ (kN) 56.07	$V_{Rd}$ (kN) 558.00	10.05%
<b>Bayonets</b>			
Compression	$N_{c,Sd}$ (kN) 86.43	$N_{c,Rd}$ (kN) 2054.54	4.21%
Flexion	$M_{Sd}$ (kN m) 86.47	$M_{Rd}$ (kN m) 381.20	22.68%
Flexure and compression combination			67.80%
Shear	$V_{Sd}$ (kN) 86.57	$V_{Rd}$ (kN) 436.00	19.86%
<b>End wall columns</b>			
Compression	$N_{c,Sd}$ (kN) 12.97	$N_{c,Rd}$ (kN) 649.05	2.00%
Flexion	$M_{Sd}$ (kN m) 36.00	$M_{Rd}$ (kN m) 54.60	65.93%
Flexure and compression combination			68.60%
Shear	$V_{Sd}$ (kN) 13.00	$V_{Rd}$ (kN) 215.00	6.05%

#### 5.2.6. Base Plates and Anchors

In this item, the results obtained in the design of the base plates will be presented, taking into account the axial force and the bending moment acting on the frame column. Therefore, it is necessary to verify each of the calculation combinations that produce the maximum efforts in the structure, in order to evaluate which one of them is the most critical load on the base plate.

For calculation purposes, the dimensions of the base plate and the diameter of the anchor bolts were pre-defined and subsequently verified. Anchor bolts have been checked for a diameter of 38.1 mm (1 ½ in) and the base plate dimensions are shown in Figure 9.

The tensile force acting on the anchors, the contact pressure on the concrete base, as well as the base plate thickness were calculated according to the method proposed by [14].

For the concrete base, it was considered a characteristic compressive strength of 30 MPa, and

the secant modulus of elasticity of the concrete equal to 27,000 MPa. One of the steps of the aforementioned method is to find the position of the neutral line through a third-degree polynomial, this position being what delimits the tensioned zone and the compressed zone of the plate. For this work, it was verified that the neutral line is 340 mm from the right end of the base plate. From this, the tensile force acting on the two anchor bolts on the left side was calculated, which was equal to 262 kN. The anchor bolts met the design request both in the verification of the yield of the gross section and in the rupture of the net section, according to item 6.3.3 of [10], which presented, respectively, design resistant tensile forces equal to 518 kN and 506 kN.

According to item 6.3.3.4 of [10], in order to verify the shear forces combined with tensile forces for threaded round bars in general, an additional limitation of the value of the tensile force requesting calculation by anchor bolt must be considered. With this, it was verified that the anchor bolts resist the shear forces acting, with no need to use a shear bar.

The length of the anchor bolts was determined according to item 9.4 of [15] and, for this, a bond strength between the anchor and the concrete of 1.31 MPa was calculated, according to item 9.3 of [15]. The anchorage length, considering the anchor bolts with hook, was calculated equal to 800 mm.

From the method of [14], the contact pressure acting on the concrete base, for this work, is equal to 7.73 MPa, while the compressive strength of the calculation of this base is 19.89 MPa, thus, the base has resistance the crushing caused by the actions

acting on the column and transmitted by the base plate.

For design the thickness of the base plate, the flexural strengths of the overhangs of this base were verified for the acting contact pressure, according to the method mentioned above. Thus, a minimum thickness of 40 mm was calculated for the base plate, however, the immediately higher commercial thickness of 44.5 mm was adopted (1 ¾ in). The details of the base plate and the anchors are shown in Fig. 9, with measurements in millimeters.

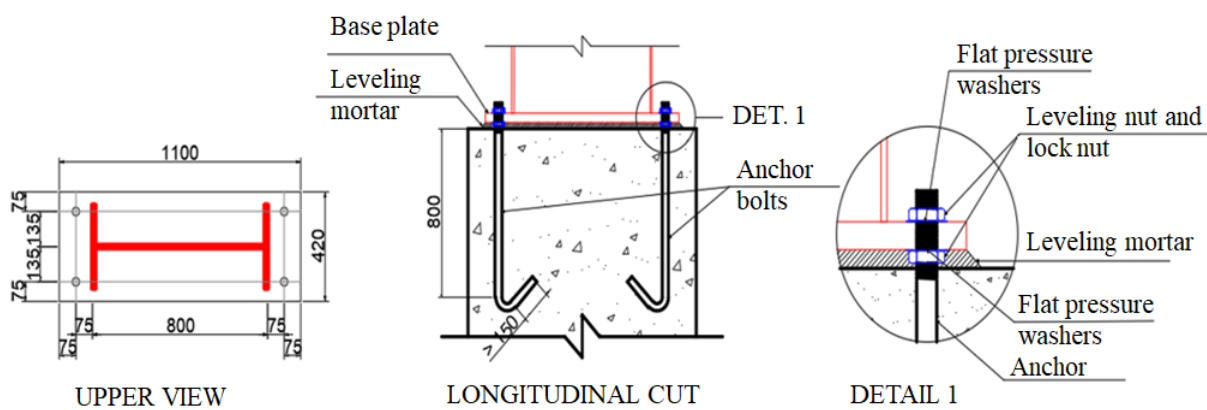


**Fig. 9: Base plate and anchors of the frame columns.**

### 5.3. STRUTS, PURLINS AND STRINGERS

The horizontal actions acting on the end wall columns are transmitted to the brace of the bottom chord of the trusses, through the struts of this same brace. In addition, the bars of the bottom chord of some trusses are part of the bracing span, for this reason, after calculating the efforts for this span, the additional requests were added in the verifications of these chords. The braces of the bottom chord bracing and the diagonals of this span were dimensioned and verified for profiles with two angles in a cross of 4 in x 1/4 in.

For the lateral bracing, the horizontal forces longitudinal to the shed also act due to the braking of the crane. As described above, the calculation model was launched in the software, and the elements were dimensioned for the requesting efforts. For the diagonals of this bracing, profiles of two 4 in x 1/4 in cross equal angles were dimensioned, and for the struts W 6 in x 22.5 kg/m profiles were dimensioned.

The purlins are subjected to bending around the two principal axes of inertia, which are checked for resistance to oblique bending, according to item 5.5.1.2 of [10], with the design resistant bending moments determined from the annex G from [10], where, for bending in the roof plane, the unlocked length is reduced due to the use of streamlines, as shown in Fig. 3. For these purlins, a laminated U-type profile of 6 in x 12.2 kg/m.

Permanent forces act on the stringers due to their own weight and the weight of the tiles, in addition to the actions of the wind in closing the shed. These elements are also subject to oblique bending, being dimensioned in the same way as the purlins and obtaining the same laminated profile of the type U of 6 in x 12.2 kg/m.

The dimensioned profiles were launched in the calculation model in SAP 2000 and the maximum displacements at each point of the structure were verified. These displacements met the requirements set out in Annex C of [10] for the serviceability limit state.

#### 5.4. BEARING BEAMS

In this item, the efforts will be presented, in addition to all the checks carried out for the bearing beam, which receives all the crane loads and part of the maintenance footbridge loads, as well as its detailing. The steel considered for design was ASTM A36.

##### 5.4.1. Soliciting Forces

According to the information presented in item 2.3 of this work, a gravitational distributed action was determined on the bearing beam of  $1.57 \text{ kN m}^{-1}$ , generating a bending moment of  $7.07 \text{ kN m}$  and a shear force of  $4.71 \text{ kN}$ . Due to the footbridge, a uniformly distributed overload of  $1.20 \text{ kN m}^{-1}$ , which causes  $5.40 \text{ kN m}$  bending moment and  $3.60 \text{ kN}$  shear force.

From what was exposed in the same item mentioned above, it was found that the moving actions of the crane generate a maximum bending moment of  $306.7 \text{ kN m}$  and a maximum shear force of  $288.6 \text{ kN}$  in the bearing beam.

All design forces requesting were determined using the last normal combinations of the aforementioned values, which generated a bending moment and a horizontal design requesting shear

force of  $36.8 \text{ kN m}$  and  $34.7 \text{ kN}$ , respectively, while the moment bending force and the design shear force acting in the vertical were equal to  $472.8 \text{ kN m}$  and  $441.4 \text{ kN}$ , respectively.

##### 5.4.2. Resistant composite section

For verification of the bearing beam, a custom welded profile  $800 \text{ mm} \times 90 \text{ kg/m}$  was considered, which should alone resist the vertical actions acting on this element. However, the beam is subject to a horizontal force, transverse due to the bearing path, which becomes worrying due to its magnitude and due to the resistance on the axis of less inertia. For this reason and to reduce the slenderness of the profile subjected to lateral-torsional buckling, a resistant composite section was considered, formed by the upper part of the bearing beam, the maintenance footbridge plate and the U profile that supports the plate on the opposite side to the beam.

To consider a resistant T section, without problems of web local buckling, the requirements for Group 6 of Table F.1 of Annex F of [10] were used, and a height for the web of the T profile considered equal to  $130 \text{ mm}$  and, from that, its geometric characteristics were determined. The representation of this composite cross section is shown in Fig. 10, with measurements in millimeters.

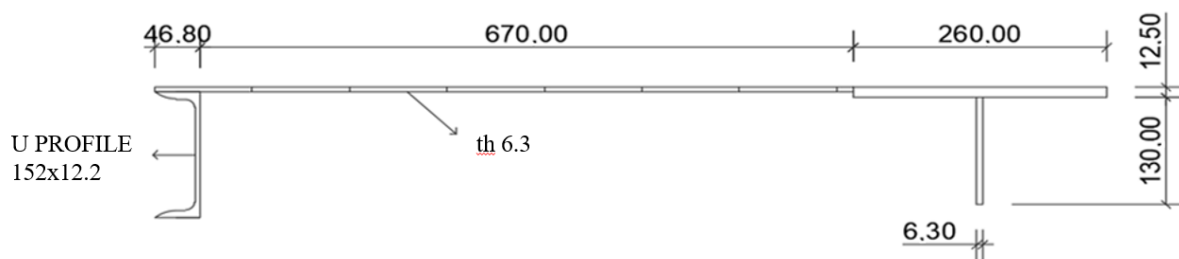


**Fig. 10: Bearing beam composite section.**

##### 5.4.3. Flexural strength

The design resistant bending moment of the bearing beam was determined in accordance with the provisions of Annex G of [10], for lateral-torsional buckling (LTB), for local flange buckling (LFB) and for local web buckling (LWB). The most critical case verified was for LWB, which presented a design resistant moment value equal to  $772 \text{ kN m}$ , which resists the design requesting bending moment of  $472.8 \text{ kN m}$ .

##### 5.4.4. Resistance to combined normal and shear stresses

The combined horizontal and vertical bending moments cause maximum stress in the upper right fiber of the beam. The longitudinal action was neglected for the calculation of the combined stresses since its value of  $49 \text{ kN}$  is negligible when compared to the normal resistant design force of  $2595 \text{ kN}$ . For this, the values of the maximum requesting stress and the design resistant stress were

found equal to 166.5 MPa and 227.2 MPa, respectively.

The design resistant shear force for the rolling beam was calculated according to item 5.4.3.1 of [10], where it was verified that the beam would not resist these forces, requiring the use of transverse stiffeners. These stiffeners were designed with an adequate spacing, with a maximum spacing of 860 mm, in addition were considered the requirements established by item 5.4.3.1.3 of [10], for which the thickness of the 8 mm (5/16 in) stiffener plate and the distance between the closest points of the welds between flange and web and between stiffener and web of 30 mm.

#### 5.4.5. Local web crippling

The ultimate limit state of crippling for the web of the bearing beam requested to compression by a localized force was verified, according to item 5.7.4 of [10]. For this verification, two cases are considered: the compressive force is at a distance from the beam end greater than or equal to half the height of the cross section, for which it was verified that there will be no crippling of the web; and the other to verify the compressive force acting in the region closest to the beam end, for which it was necessary to increase the web thickness to 8 mm (5/16 in).

#### 5.4.6. Web local buckling and yielding due to concentrated load

Item 5.7.6 of [10] determines the verification of the web local buckling requested by compression of a pair of forces located in opposite directions, this condition being verified in the supports of the bearing beam, for which the need to use of a support stiffener, since the design force of 441.4 kN is greater than the design resistance force, for this condition, of 50.9 kN.

The support stiffeners were dimensioned to resist the compressive stress due to the concentrated load according to item 5.3 and fulfilling the requirements of item 5.7.9, both of [10]. Thus, a 260 mm wide and 9.5 mm (3/8 in) thick support stiffener plate was assigned.

In addition to these verifications mentioned above, the bearing beam was verified for the web local yielding, according to item 5.7.3 of [10], from which a design resistant force of 7714 kN was obtained, which fulfills the calculation request.

#### 5.4.7. Fatigue check

The verification regarding the fatigue of the bearing beam was carried out in accordance with the criteria established in Annex K of [10], with a number of cycles equal to 2,000,000 for a period of use of 50 years. Since, for the lower flange, the stress variation is equal to 97.8 MPa, having an admissible range of stress variation of 124.5 MPa, while, for the transverse stiffeners, the variation of stresses is equal to 87.4 MPa and the allowable range for this is 89 MPa.

#### 5.4.8. Composition welds and beam detailing

The welds of welded profiles are calculated as a function of the longitudinal shear stress in the web and local stresses. For the weld between the web and the upper flange, a full penetration weld was considered and the stresses acting on the weld were calculated: due to shear, equal to 71.4 MPa; due to the concentrated load of the crane wheel, equal to 179.2 MPa; and due to the acting bending moments of 162.1 MPa. Generating a resultant stress in the weld of 211.2 MPa, which is lower than the design resistant stress, defined in item 6.2 of [10], equal to 227.2 MPa.

For the design of the weld between the web and the lower flange, a fillet weld was considered, using the minimum size of the depth weld, established in item 6.2.6.2.1 of [10] of 5 mm. The maximum stress variation was calculated equal to 42.1 MPa, being within the permissible range of stress variation, calculated equal to 55 MPa, according to Annex K of [10].

The detailing of the bearing beam with all its elements verified in this work is shown in Fig. 11, with measurements in millimeters.

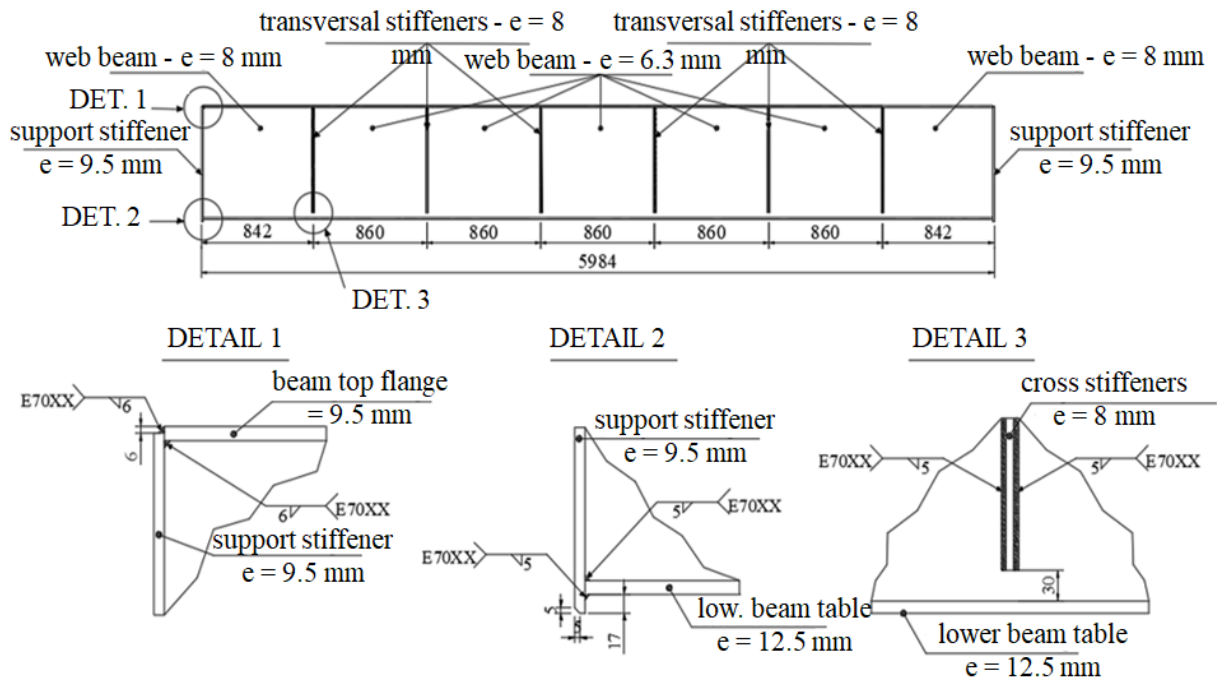


**Fig. 11: Bearing beam detailing.**

### 5.5. FRAME DESIGN FOR SERVICEABILITY

After designing the profiles of all the components of the shed's frames, they were modeled in the analysis software, and the maximum displacements were verified at some specific points. Table 8 shows the values of the horizontal displacements for the top of the frame column, the top of the bearing beam, the level of the bottom chord and the level of the top chord. In addition to the vertical displacement of the midpoint of the roof

truss and the relative displacement between the two columns where the bearing beam is supported, compared to the maximum values for such displacements, established by Table C.1 of Annex C of [10], while Fig. 12 shows the most critical deformation profile of the gantry, obtained from the SAP 2000 software, with the lateral color scale in millimeters.

Table 8: Maximum displacements in the frame - SLS.

Position	$\delta$ (mm)	$\delta_{\max}$ (mm)	Profile Use
Top of column	22	23	95.65%
Bearing beam top	23	25	92.00%
Bottom chord level	29	40	72.50%
Top chord level	31	43	72.09%
Trusses midpoint	30	40	75.00%
Relative between columns	5	15	33.33%

being,  $\delta$  is the most critical displacement generated by combinations of actions;  $\delta_{\max}$  is the maximum displacement value established by Annex C of [10].

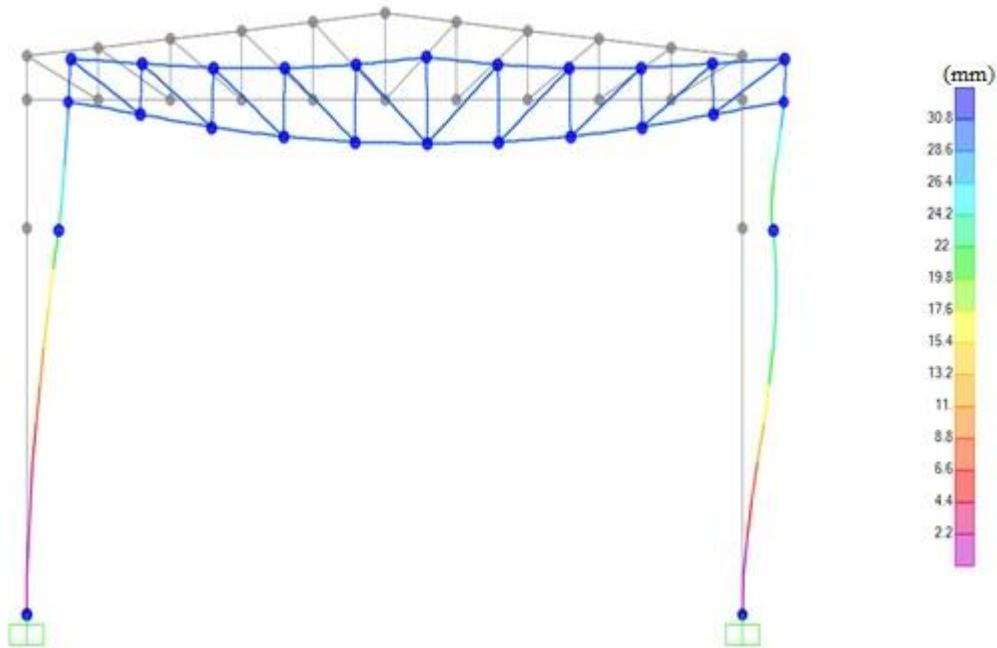


**Fig. 12: Maximum displacement of the frame.**

### 5.6. CONNECTIONS

This item shows the connections between the bottom chord of the trusses and the bayonet and between the top chord and the bayonet.

#### 5.6.1. Bottom chord-bayonet connection

For the Bottom chord-bayonet connections, centered shear flexible connections were used. It was

decided to use a connecting plate welded to the bayonet flange and screwed to the double angles, using ASTM A36 steel for the plates, ASTM A325 for the screws and E70 electrode for the weld. The connection checks were carried out in accordance with items 6.2 and 6.3 of [10] and the details of this connection are shown in Fig. 13, with measurements in

millimeters.

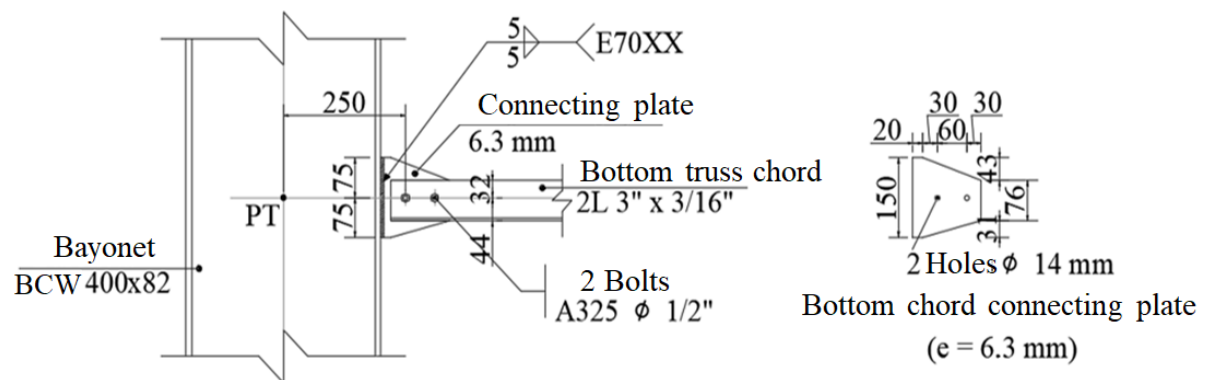


**Fig. 13: Bottom chord-bayonet connection.**

#### 5.6.2. Top chord-bayonet connection

Flexible connections were also used for the top chord-bayonet connections, however, in this case,

the weld is subject, in addition to shear due to vertical and horizontal stresses, to shear due to the bending moment caused by the eccentricity between the axes of action of the stresses and the center of

gravity of the weld. In this case, a connection plate was also used, using the same characteristics of the connection in the previous item. The details of this

connection are shown in Fig. 14, with measurements in millimeters.

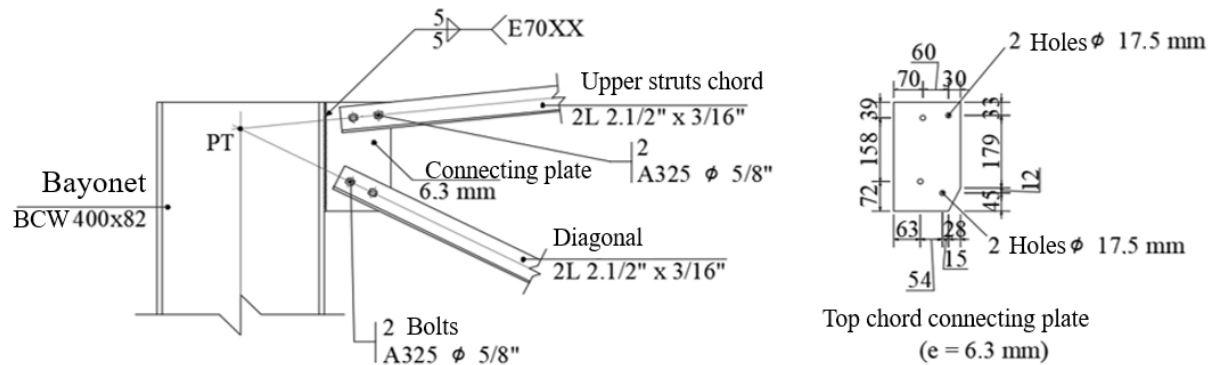


**Fig. 14: Top chord-bayonet connection.**

## VI. CONCLUSIONS

Through the results obtained in this work, it is possible to demonstrate the importance of analyzing all the checks established by the technical standards, to obtain an economic project, but above all, safe. If all checks are not carried out, the replacement with a lighter profile could erroneously occur, which would result in a false economy, since the structure would not be safe, because, as observed, for the steel profile dimensioned in this work, for the verifications regarding the flexure and compression and regarding the maximum displacements in the service limit state, presented percentages of utilization of 68% and 96%, respectively. It was observed that the highest percentage of utilization of the column profile is due to displacements, which is due to the magnitudes of the horizontal force transverse to the rolling path, caused by the overhead crane. Therefore, a lighter profile would not meet such requests.

Another important factor was observed in the design and verification of the bearing beam, in which the defined profile did not fulfill some of the requests, but some alternatives solutions utilized allowed the structural element to fulfill all the established criteria, without the need to use a profile more robust, making the project more economical and keeping it safe. In view of this, the structural system chosen for the shed under study proved to be adequate, fulfilling all the recommended normative checks.

Future research can contribute to the expansion of the analyzes developed in this research, such as

the dimensioning and detailing of all connections; the preparation of the list of materials; the definition of the type of tile, gutters and side closure material; and the elaboration of the fabrication and assembly project.

## ACKNOWLEDGMENTS

The authors thank the Foundation for the Support of Science and Technology of Pernambuco (FACEPE), the Pro-Rectorry of Graduate Studies (PROPG) and the Coordination of Superior Level Staff Improvement (CAPES), for funding the research developed in the Graduate Program in Civil and Environmental Engineering (PPGECAM) of the Federal University of Pernambuco (UFPE) at the Caruaru Campus.

## REFERENCES

- [1] L. C. dos Passos, *Apostila: Técnicas de instalação, operação, manutenção testes e inspeção: pontes rolantes, guindastes giratórios e acessórios de movimentação de cargas (Make Engenharia, Acessoria e Desenvolvimento, Brasil, 2011).*
- [2] G. Sordi, *Dimensionamento da Viga Principal de uma Ponte Rolante (Centro Universitário Univantes, Lajeado, 2016).*
- [3] N. B. Almutairi, and M. Zribi, Sliding Mode Control of a Three-dimensional Overhead Crane (*Journal of Vibration and Control*, v. 15, Issue: 11, p. 1679-1730, 2009).
- [4] Wu, X., and He. X. Partial feedback linearization control for 3-D underactuated overhead crane systems (*ISA Transactions*, v. 65, p. 361-370, 2016).

- [5] R. Kubicki, and M. Mrówczyńska, Assessment of the Straightness Condition of the Overhead Crane Trestle in a Steel Structure (*Quarterly of Environmental Engineering and Design*, v. 171, Issue: 51, p. 64-72, 2018).
- [6] H. Chen, B. Xuan, P. Yang, and H. Chen, A new overhead crane emergency braking method with theoretical analysis and experimental verification (*Nonlinear Dyn.*, v. 98, p. 2211–2225, 2019).
- [7] P. Lehner, M. Krejsa, P. Pařenica, V. Křivý, and J. Brožovský, Fatigue damage analysis of a riveted steel overhead crane support truss (*International Journal of Fatigue*, v. 128, 105190, 2019).
- [8] Q. Wu, X. Wang, L. Hua, and M. Xia, Dynamic analysis and time optimal anti-swing control of double pendulum bridge crane with distributed mass beams (*Mechanical Systems and Signal Processing*, v. 144, 106968, 2020).
- [9] Q. Qi, Y. Yu, Q. Dong, G. Xu, and Y. Xin, Lightweight and green design of general bridge crane structure based on multi-specular reflection algorithm (*Advances in Mechanical Engineering*, v. 13, Issue: 10, p. 1-15, 2021).
- [10] NBR 8800, Projeto de estruturas de aço e de estruturas mistas de aço e concreto de edifícios, *Associação Brasileira de Normas Técnicas* (Rio de Janeiro, 2008).
- [11] NBR 6123, Forças devidas ao vento em edificações, *Associação Brasileira de Normas Técnicas* (Rio de Janeiro, 1988).
- [12] G. QUEIROZ, *Elementos das estruturas de aço* (Belo Horizonte, 1986).
- [13] K. MUKHANOV, *Estruturas metálicas*. (Editora MIR, Moscou, 1980).
- [14] J. M. FISHER, and L. A. KLOIBER, Base Plate end Anchor Rod Design - Steel Design Guide 1. 2<sup>a</sup> ed. (*American Institute of Steel Construction*, Chicago, 2006).
- [15] NBR 6118, Projeto e Execução de Obras de Concreto Armado, *Associação Brasileira de Normas Técnicas* (Rio de Janeiro, 2014).